

# Assessment of Planetary Boundary-Layer Schemes in the Weather Research and Forecasting Mesoscale Model Using MATERHORN Field Data

Reneta Dimitrova<sup>1,2</sup> · Zachariah Silver<sup>1</sup> · Tamas Zsedrovits<sup>1,3</sup> · Christopher M. Hocut<sup>1,4</sup> · Laura S. Leo<sup>1</sup> · Silvana Di Sabatino<sup>1,5</sup> · Harindra J. S. Fernando<sup>1</sup>

Received: 8 September 2014 / Accepted: 22 September 2015 / Published online: 7 October 2015  
© Springer Science+Business Media Dordrecht 2015

**Abstract** The study was aimed at understanding the deficiencies of numerical mesoscale models by comparing predictions with a new high-resolution meteorological dataset collected during the Mountain Terrain Atmospheric Modelling and Observations (MATERHORN) Program. The simulations focussed on the stable boundary layer (SBL), the predictions of which continue to be challenging. High resolution numerical simulations (0.5-km horizontal grid size) were conducted to investigate the efficacy of six planetary boundary-layer (PBL) parametrizations available in the advanced research version of the Weather Research and Forecasting model. One of the commonly used PBL schemes was modified to include eddy diffusivities that account for enhanced momentum transport compared to heat transport in the SBL, representing internal wave dynamics. All of the tested PBL schemes, including the modified scheme, showed a positive surface temperature bias. None of the PBL schemes was found to be superior in predicting the vertical wind and temperature profiles over the lowest 500 m, however two of the schemes appeared superior in capturing the lower PBL structure. The lowest model layers appear to have a significant impact on the predictions aloft. Regions of sporadic flow interactions delineated by the MATERHORN observations were poorly predicted, given such interactions are not represented in typical PBL schemes.

**Keywords** Boundary-layer parametrization · Complex terrain · Stable boundary layer · Turbulence · Weather Research and Forecasting model evaluation

---

✉ Reneta Dimitrova  
Reneta.Dimitrova@nd.edu; rdimitrova@geophys.bas.bg

<sup>1</sup> Civil and Environmental Engineering and Earth Sciences, University of Notre Dame, Notre Dame, IN 46556, USA

<sup>2</sup> Atmospheric Physics - Department of Geophysics, National Institute of Geophysics, Geodesy and Geography, Bulgarian Academy of Sciences, 1113 Sofia, Bulgaria

<sup>3</sup> Faculty of Information Technology and Bionics, Pazmany Peter Catholic University, Budapest 1088, Hungary

<sup>4</sup> U.S. Army Research Laboratory, White Sands Missile Range, NM 88022, USA

<sup>5</sup> Department of Physics and Astronomy, University of Bologna, Bologna, Italy

## 1 Introduction

The parametrization of subgrid-scale boundary-layer processes continues to be a challenge for mesoscale numerical weather prediction models. Parametrization schemes quantify the contribution of numerically unresolved atmospheric processes in terms of variables resolved at the model's discrete grid. Efforts to improve planetary boundary-layer (PBL) parametrizations have mainly followed two approaches: (1) those that assess the validity of assumptions underlying the parametrization schemes and their adequacy in representing natural flows (Mellor and Yamada 1982; Zhang and Anthes 1982; Bougeault and Lacarrere 1989; Janjic 1990, 1994, 2002; Grell et al. 1994; Hong and Pan 1996; Alapaty et al. 1997; Sukoriansky et al. 2005; Hong et al. 2006; Lee et al. 2006; Pleim 2006, 2007a,b; Sukoriansky 2008; Jiménez et al. 2012), and (2) those devoted to comparing predictions based on existing parametrization schemes for different environmental settings (Braun and Tao 2000; Stensrud and Weiss 2002; Bright and Mullen 2002; Zhang and Zheng 2004; Lee and Fernando 2004; Deng and Stauffer 2006; Fernández et al. 2007; Otkin and Greenwald 2008; Reeves and Stensrud 2009; Hu et al. 2010; Argüeso et al. 2011; Awan et al. 2011; Evans et al. 2011; Flaounas et al. 2011; Shin and Hong 2011; Garcia-Diez et al. 2013; LeMone et al. 2013). Studies of the first kind are aimed at delineating missing or under-represented processes and including them more accurately into the models. The second kind adopts a more pragmatic approach, for example, the selection of the best scheme for a given purpose and setting (e.g., weather forecasts for a specific region or phenomenon; regional climate research). Both approaches require comprehensive datasets, not only detailed point measurements at standard meteorological heights, but also profiling data at different locations. This is evident in the work of Zhong and Fast (2003).

Several studies have focused on selecting appropriate model configurations. In particular, parametrizations for various conditions and applications have been examined by using the Weather Research and Forecasting (WRF) model (<http://www.mmm.ucar.edu/wrf/users>). A number of different combinations of microphysical and PBL parametrization schemes were exploited by Jankov et al. (2007) and Otkin and Greenwald (2008). Diverse cumulus schemes have been tested in addition to physical options used in the works cited above (Li and Pu 2008; Argüeso et al. 2011; Flaounas et al. 2011). Twenty-three alternative model configurations were invoked in Borge et al. (2008), and which included: PBL schemes, microphysics, land-surface models, radiation schemes, sea-surface temperature and four-dimensional data assimilation. Awan et al. (2011) and Evans et al. (2011) investigated the role of physical parametrizations in regional climate simulations using a mixed physics ensemble in the WRF model; the accuracy could not be uniquely attributed to a single parametrization but to the combination of parametrizations selected, as a result of the strong non-linearity of the governing equations. The influences of synoptic conditions were considered under various conditions such as: rainfall events (Jankov et al. 2007; Evans et al. 2011; Flaounas et al. 2011), early rapid intensification of hurricanes (Li and Pu 2008) and extratropical cyclones (Otkin and Greenwald 2008), as well as strong synoptic forcing (Zhang et al. 2013).

A number of studies have focused on optimal PBL parametrization suited to a given purpose. For example, the sensitivity of the WRF model simulations to the Mellor–Yamada–Janjic (MYJ) scheme, the Yonsei University (YSU) scheme and the asymmetric convective model—version 2 (ACM2) scheme were examined by Hu et al. (2010). Their model domain covered eastern Texas, western Louisiana, and a part of Arkansas to simulate conditions during July–September 2005. Simulations with the YSU and ACM2 schemes yielded a much smaller bias than those performed with the MYJ scheme. Simulations with a variety of PBL

schemes were conducted by [García-Díez et al. \(2013\)](#) with a domain covering Europe for a 1-year period. The three PBL schemes used were evaluated based on temperature, specific humidity, and the PBL height. [Shin and Hong \(2011\)](#) simulated meteorological fields using five PBL schemes for a single day of the Cooperative Atmosphere-Surface Exchange Study field program. Two first-order closure schemes (YSU and ACM2 schemes) and three turbulent kinetic energy (TKE) closure schemes (MYJ, quasi-normal scale elimination (QNSE), and Bougeault–Lacarrère (BouLac) schemes) were used. The best scheme for simulating the convective boundary layer (CBL) was found to be a non-local scheme with the entrainment flux proportional to the surface flux. Under stable conditions, however, the schemes that use a local TKE closure performed better. [LeMone et al. \(2013\)](#) tested eight objective methods to identify the CBL height  $H_{\text{cbl}}$  using four PBL schemes: YSU, MYJ, BouLac and QNSE. In the case of the BouLac, MYJ, and QNSE schemes with a 1-km or a 3-km grid, the TKE thresholds performed poorly and  $H_{\text{cbl}}$  showed an irregular growth. The local TKE closure schemes in general underestimated the  $H_{\text{cbl}}$  value. The WRF model performance for near-surface temperature and wind predictions for weather regimes and terrain was studied by [Zhang et al. \(2013\)](#). As for the weather regime, cases with a low-level jet and a persistent inversion were evaluated against Mesonet observational data, and good agreement between model and observations was noted for near-surface variables over flat terrain. For complex terrain, the model predictions were poor, in part due to inability of representing the actual terrain. The forecast errors for the near-surface variables were found to depend on the diurnal variation of surface conditions, in particular, when the synoptic forcing is weak. Under strong synoptic forcing, the diurnal patterns of the errors disappeared, highlighting flow-dependent errors. [Kleczek et al. \(2014\)](#) evaluated six PBL schemes (YSU, ACM2, MYJ, Mellor–Yamada Nakanishi and Niino Level 2.5 (MYNN), QNSE, and BouLac schemes) for a relatively flat area surrounded by grassland, fields, tree lines, and scattered villages; non-local schemes produced higher temperatures and wind speeds than local schemes, particularly at night.

The present study was motivated by the availability of a new high resolution dataset from the Mountain Terrain Atmospheric Modelling and Observations (MATERHORN) Program ([Fernando and Pardyjak 2013](#); [Fernando et al. 2015](#)) to assess PBL schemes within the advanced research version of the WRF model. The focus is to evaluate the model capability of capturing thermally-driven flows in complex terrain under weak synoptic conditions. The most challenging, and hence of particular interest, is the stable boundary layer (SBL) that includes notoriously elusive physics of stratified turbulence, non-linear internal waves, sharp transitions and even phase changes such as fog formation ([Fernando and Weil 2010](#); [Mahrt 2010](#); [Mahrt et al. 2012](#)). Forecasts of complex terrain weather are also predicated on the interaction of slope and valley flows and their interactions with synoptic flow ([Fernando and Pardyjak 2013](#)). Another complication is the difficulty of accurately representing the local terrain ([Wagner et al. 2014](#)).

In the present work, high resolution (0.5-km horizontal grid spacing) WRF model simulations were conducted to evaluate the capabilities and limitations of commonly used PBL parametrization schemes for dry, stably stratified nocturnal periods. In addition, considering the merits of the YSU scheme for convective conditions ([Hu et al. 2010](#); [Shin and Hong 2011](#); [LeMone et al. 2013](#); [Kleczek et al. 2014](#)), a semi-empirical model of [Monti et al. \(2002\)](#) for the eddy diffusivities of heat and momentum was implemented therein for stable conditions as a possible improvement. The modified scheme was evaluated alongside of the existing scheme. This semi-empirical model has been implemented in the medium range forecast (MRF) scheme ([Hong and Pan 1996](#)) within the Pennsylvania State University/National Center for Atmospheric Research mesoscale model ([Grell et al. 1994](#)), known as MM5, and

the results show promising improvements to nocturnal near-surface air temperature predications and a slight improvement to wind-speed predictions (Lee et al. 2006).

The present work complements previous PBL scheme evaluation studies in several ways; it utilizes a new comprehensive dataset from the MATERHORN experiments taken at an unprecedented spatio-temporal detail, and it modifies the YSU PBL scheme for stable conditions with a semi-empirical eddy-diffusivity model.

## 2 Observations

The MATERHORN experiments were conducted in the Great Salt Lake Desert at the U.S. Army Dugway Proving Grounds (DPG) in a region surrounded on three sides by mountain ranges ([www.nd.edu/~dynamics/materhorn](http://www.nd.edu/~dynamics/materhorn)). The Granite Mountain Atmospheric Sciences Testbed is centred on a single mountain (Granite mountain within DPG) with the following core instrumentation arranged in an array: 31 Surface Atmospheric Measurement Systems (SAMS), 51 mini-SAMS and over 100 Portable Weather Instrumentation Data Systems (PWIDS). The SAMS and mini-SAMS are 10-m towers with vane anemometers at 2 and 10 m above ground level used to measure wind speed and direction, as well as temperature and relative humidity at 2-m height. The PWIDS are portable masts on tripods with a vane anemometer and a temperature/relative humidity probe at 2 m. This core infrastructure was augmented with an extensive suite of instrumentation concentrated at five Intensive Observing Sites with towers, at least 20 m in height, along with a set of specialized sensors. A full description of all instruments and site locations is given in Fernando et al. (2015).

During the quiescent (wind speed  $< 5 \text{ m s}^{-1}$  at 700-hPa height) intense operational periods (IOP), special attention was given to the interaction between the downslope flow, along the east slope of Granite mountain, and the valley flow to the east of the mountain along the Dugway valley. Continuous tethered-balloon flights were launched at the Sage Brush (SB) site, which was centrally located in the valley. In addition, a line of four towers (ES2, ES3, ES4, and ES5) was installed that extended from the slope base onto the east slope of the mountain. The ES2 tower was located furthest to the east at the slope base, while the ES5 tower was located furthest to the west at the highest elevation (Fig. 1b, c).

## 3 Model Set-up

The simulations were performed using the advanced research version of the WRF model (ARW-WRFv3.4.1, released on August 16 2012), a state-of-the-art mesoscale numerical weather prediction system, suitable for a broad range of applications, including parametrized physics. The system solves the fully compressible, non-hydrostatic Euler and scalar conservation equations, with the upper boundary of the model at a constant pressure surface and the vertical coordinate used is based on a terrain-following approach with the possibility of vertical grid stretching.

### 3.1 Modelling Domains

Four nested domains of 32-, 8-, 2- and 0.5-km horizontal grids were used, based on a Lambert projection centred at 113°W, 40°N (located in Utah, USA). The experimental domain is shown in Fig. 1, with the vertical grid set to 50 terrain following (*eta*) levels based on preliminary evaluation of the model with a total of 50, 40 and 35 levels. More points were

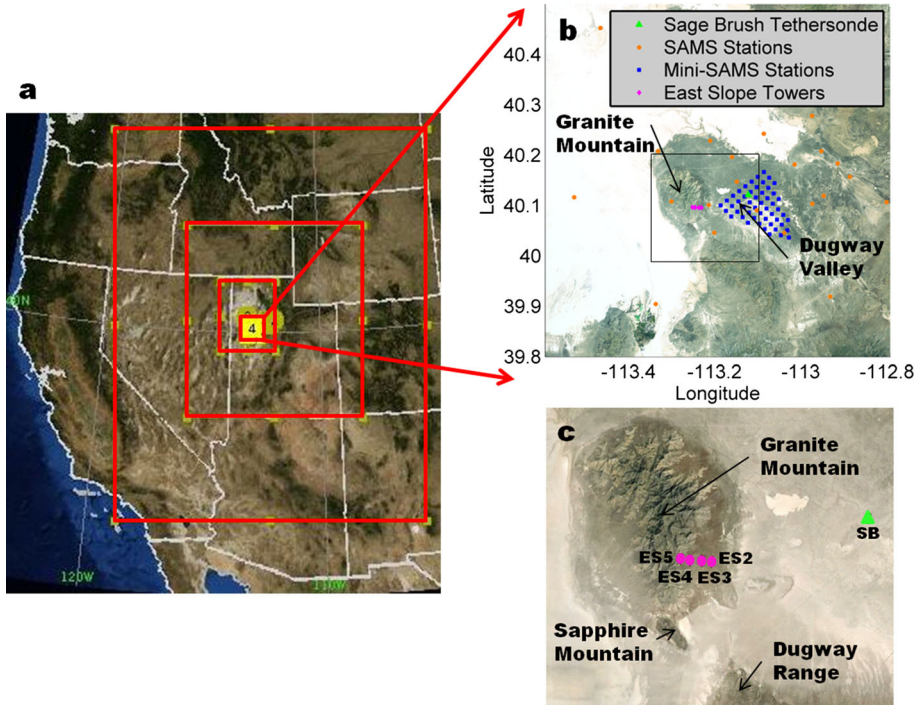


**Fig. 1** Model domains for the numerical simulations (a), domain D4 with 0.5-km grid (b) including locations of the instruments used for model evaluation, and Granite mountain area (c)

employed in the lowest part of the PBL to increase the vertical resolution. For example, 22, 15 and 11 levels respectively, were selected below 600 m with gradually increasing distance between the levels. The model top was set to 5000 Pa. Multiple domains at different grid spacing were run simultaneously in one-way interactive nested simulations to investigate the effect of horizontal resolution on the model simulations (see Sect. 4.2). The coarser domain provided boundary conditions for the nest.

The initial and boundary conditions (for the parent domain) are based on the National Centers for Environmental Prediction Final Operational Model Global Tropospheric Analyses (<http://rda.ucar.edu/datasets/ds083.2/>), which is a product of the Global Data Assimilation System that continuously collects observational data from the Global Telecommunications System. In 2012, the land-cover and terrain elevation dataset was updated based on the newer 33-category national land-cover database (Fry et al. 2011), which includes the new land-cover area defined as playa (dry lake bed); this is shown in Fig. 1b. The properties of playa are quite distinct from other desert and non-desert substrates, and the resulting land-use mosaic produces a playa breeze unique to desert environments. The breeze forms around the edge of the playa as a result of differential heating (Rife et al. 2002). The soil-texture class is defined by a 16-category United States Geological Survey (USGS) dataset, which is also modified to include playa, white sand, and lava soil texture classes. The updated database was used together with a new parametrization of soil thermal conductivity in the Noah land-surface model for silt loam and sandy loam soils. The latter modification was proposed by Massey et al. (2013), which significantly reduced the nocturnal temperature bias. No data assimilation was applied in our study, in contrast to Massey et al. (2013).

### 3.2 Modelling Periods

Data from autumn 2012 (September 25–October 21) and spring 2013 (May 1–30) MATERHORN field campaigns were used. The autumn observational program focused on thermal circulation under quiescent, synoptic anticyclonic background conditions, while the spring campaign concerned periods of strong synoptic flow (Fernando et al. 2015) although some quiescent periods were observed. The present study covers six quiescent IOPs selected from both campaigns, which include:

Autumn 2012:

IOP1 (28 September 1400–29 September 1400), IOP2 (01 October 1400–02 October 1400), IOP6 (14 October 0200–15 October 0200), IOP8 (18 October 0500–19 October 1200);

Spring 2013:

IOP4 (11 May 1400–12 May 1400), IOP7 (20 May 1715–21 May 1400).

IOPs typically extended over 24-h periods, with the exception of IOP8 (31 h) and IOP7 (21 h). The listed time is local (UTC–6 h). All numerical simulations cover 48-h segments; a sufficient spin-up time (12 h or more, depending on the IOP starting time) was allowed prior to the selected time period for comparison with field data.

### 3.3 Physical Parametrizations

The WRF model physical parametrizations include the following: microphysical scheme (Lin et al. 1983), the rapid radiative transfer model longwave radiation parametrization (Mlawer et al. 1997), the Dudhia shortwave radiation parametrization (Dudhia 1989), and the Noah land-surface model (Chen and Dudhia 2001). Most of the available PBL schemes in the ARW-WRFv3.4.1 model version were considered, which are: the Yonsei University scheme, YSU (Hong et al. 2006), the Asymmetric Convective Model, version 2 scheme, ACM2 (Pleim 2007a), the Mellor–Yamada–Janjic scheme, MYJ (Janjic 1990), the Mellor–Yamada–Nakanishi–Niino Level 2.5 scheme, MYNN (Nakanishi and Nino 2006), the Bougeault and Lacarrere scheme, BouLac (Bougeault and Lacarrere 1989), and the Quasi-Normal Scale Elimination scheme, QNSE (Sukoriansky et al. 2005).

The YSU scheme is a non-local first-order scheme with explicit treatment of entrainment processes at the top of the PBL. To allow for non-local vertical fluxes, a term is added to the turbulent diffusion equations for prognostic variables, while the PBL height is estimated using a critical bulk Richardson number approach. The other first-order scheme used is the ACM2 scheme, which is a combination of the local and non-local mixing approaches (explicit non-local upward mixing and local downward mixing). The ACM2 scheme removes non-local transport and uses local closure for stable and neutral conditions.

The remaining PBL schemes (MYJ, MYNN, BouLac and QNSE) are all TKE closure schemes. Only local transport is allowed, and the diffusivity is expressed as a multiplication of the mixing length scale, the square root of the TKE, and a proportionality coefficient. The definitions of the mixing length scale and proportionality coefficient, however, vary with the scheme. The QNSE scheme is an alternative to the Reynolds stress scheme, deriving momentum and heat eddy diffusivities using a self-consistent, quasi-normal scale elimination algorithm and spectral space representation.

Each PBL scheme is coupled with a surface-layer scheme, which provides the friction velocity and exchange coefficients for calculation of the surface heat and moisture fluxes via the land-surface models. These fluxes, in turn, provide a lower boundary condition for vertical transport in the PBL schemes.

The simulations with the YSU scheme were performed with the revised MM5 similarity scheme (Jiménez and Dudhia 2012; Jiménez et al. 2012). For the MYJ scheme and the BouLac scheme, the Eta similarity surface-layer scheme (Janjic 1990, 1994) was used. The other three schemes were coupled with exclusive surface-layer schemes developed: the Pleim-Xiu scheme (PX) (Pleim 2006), the MYNN scheme (Nakanishi and Nino 2006) and the QNSE scheme (Sukoriansky 2008), respectively. All five surface-layer schemes are based on Monin–Obukhov similarity theory—MOST (Monin and Obukhov 1954; Monin and Yaglom 1965), however profile functions and empirical parameters differ for different parametrization schemes.

### 3.4 Modification of the YSU Scheme for Stable Stratification

The advantages of the YSU scheme are its simplicity, general reliability and adaptability for different conditions. It is computationally inexpensive, and an improvement in predicting the CBL as compared to the schemes that adopt local closures (see the Introduction). For stable conditions (bulk Richardson number  $> 0$ ), the YSU scheme uses identical profile functions for momentum and heat, assuming a constant turbulent Prandtl number ( $Pr_t$ ). This aspect could be improved in the knowledge that experimental data (e.g., Strang and Fernando 2001a; Monti et al. 2002) show that both momentum and heat diffusivities are stability (i.e. gradient Richardson number  $Ri$ ) dependent. Monti et al. (2002) have suggested a semi-empirical model for the eddy diffusivities of heat ( $K_h$ ) and momentum ( $K_m$ ) under stable conditions, based on data obtained during the Vertical Transport and Mixing eXperiment (Doran et al. 2002). It was shown that for predominantly stably-stratified slope flows,  $K_h/K_m \approx 1$  for  $Ri < 0.2$ , indicating that stratification effects are of minor importance for such Richardson numbers and turbulent eddies transport heat and momentum with equal efficiency. At  $Ri > 0.2$ , increasing buoyancy effects reduce vertical mixing, leading to  $K_m > K_h$ , since under strongly stable stratification momentum is transferred by internal gravity waves that sustain only a small (or in the case of linear waves, no) heat flux. For  $1 < Ri < 10$ , both diffusivities only weakly depend on  $Ri$ . These results are in general agreement with the laboratory study of stratified turbulence by Strang and Fernando (2001a, b). Empirical best fits to data show the following relations, based on normalization using appropriate scales—the r.m.s. vertical velocity  $\sigma_w$  (Hunt 1985; Pearson et al. 1983) and the shear length scale  $\sigma_w |d\mathbf{V}/dz|^{-1}$  (Fernando 2003), where  $\mathbf{V}$  is the velocity vector,

$$K_m = 0.34 Ri^{-0.02} \sigma_w^2 |d\mathbf{V}/dz|^{-1}, \quad (1)$$

$$K_h = 0.08 Ri^{-0.49} \sigma_w^2 |d\mathbf{V}/dz|^{-1}. \quad (2)$$

Note that in Eqs. 1 and 2, the momentum diffusivity is larger than that of heat at high  $Ri$ . Lee et al. (2006) combined Eqs. 1 and 2 with the empirical relation of Stull (1988) to diagnostically calculate the vertical wind variance,

$$\sigma_w^2 = \overline{w'^2} = 2.5 u_*^2 [1 - (z/h)^{0.6}], \quad (3)$$

where  $h$  is the height of the mixed layer and  $u_*$  is the surface friction velocity. As already mentioned, this semi-empirical model has been implemented in the MRF PBL scheme of the MM5v3.7 model version. The YSU PBL scheme is a modified and improved version of the MRF scheme, which explicitly considers the effects of entrainment process near the PBL top. In the present study, the same parametrization (Eqs. 1–3) is implemented in the YSU PBL scheme of the ARW-WRFv3.4.1 model version (hereafter YSUmod).

## 4 Modelling Results

Simulations were performed for each of the IOPs using the six PBL schemes noted above and the modified scheme YSUmod. With several simulations conducted to assess the model sensitivity to the number of vertical levels and horizontal grid resolution, the model performance was evaluated using standard statistical measures.

### 4.1 PBL Experiment

The comparison of modelling results with field data is based on the so-called surface and vertical statistics. The SAMS and mini-SAMS data at 2 m for temperature and 10 m for wind speed were used to calculate the surface statistics (Table 1). The vertical statistics (Table 2) were obtained using tethered-balloon profiles at the SB site. This site is in the path of the Dugway basin valley flow, although at times it was disturbed by slope flows draining from either side of the valley. The vertical statistics were calculated for four IOPs by extracting the model data at the SB site to compare with measurements at selected heights above the ground. The nearest profile data from the model and balloon were interpolated to selected levels for further statistical evaluation. The root-mean-square error (*RMSE*), index of agreement (*IA*) and correlation coefficient (*r*) for temperature and wind speed are listed in Tables 1 and 2. The *IA* parameter developed by Willmott (1981) is a standardized method to determine the degree of the model prediction error

$$IA = 1 - \frac{\sum_{i=1}^N (P_i - O_i)^2}{\sum_{i=1}^N (|P_i - \bar{O}| + |O_i - \bar{O}|)^2}, \tag{4}$$

where  $P_i$  and  $O_i$  are the predicted and observed values, respectively, and  $\bar{O}$  is the mean observed value. The *IA* values range between zero and 1, with 1 indicating a perfect match. The

**Table 1** Summary of surface statistics for different PBL schemes

	ACM2	BouLac	MYJ	MYNN	QNSE	YSU	YSUmod
Temperature							
<i>RMSE</i>	4.9	5.3	5.2	5.2	4.7	5.5	5.9
<i>IA</i>	0.89	0.86	0.88	0.87	0.90	0.85	0.83
<i>r</i>	0.85	0.84	0.85	0.83	0.86	0.83	0.82
Zonal wind component							
<i>RMSE</i>	1.7	1.7	1.8	1.7	1.7	1.8	1.8
<i>IA</i>	0.74	0.74	0.73	0.72	0.76	0.70	0.72
<i>r</i>	0.56	0.55	0.53	0.54	0.58	0.49	0.51
Meridional wind component							
<i>RMSE</i>	1.8	1.9	1.9	1.8	2.0	2.0	2.2
<i>IA</i>	0.83	0.83	0.81	0.82	0.80	0.79	0.77
<i>r</i>	0.69	0.69	0.67	0.67	0.67	0.63	0.61
Wind speed							
<i>RMSE</i>	1.6	1.6	1.7	1.6	1.8	1.7	1.8
<i>IA</i>	0.72	0.74	0.70	0.71	0.64	0.67	0.66
<i>r</i>	0.51	0.54	0.47	0.49	0.39	0.43	0.42



**Table 2** Summary of vertical statistics for different PBL schemes

	ACM2	BouLac	MYJ	MYNN	QNSE	YSU	YSUmod
Temperature							
<i>RMSE</i>	1.9	1.9	1.7	1.9	1.6	2.1	2.5
<i>IA</i>	0.97	0.97	0.97	0.97	0.98	0.96	0.94
<i>r</i>	0.95	0.95	0.96	0.95	0.97	0.94	0.92
Zonal wind component							
<i>RMSE</i>	2.1	1.9	2.2	2.1	2.0	2.1	2.0
<i>IA</i>	0.60	0.61	0.60	0.60	0.61	0.61	0.61
<i>r</i>	0.37	0.39	0.36	0.37	0.37	0.38	0.38
Meridional wind component							
<i>RMSE</i>	2.4	2.0	2.5	2.3	2.4	2.4	2.1
<i>IA</i>	0.75	0.78	0.74	0.76	0.75	0.75	0.79
<i>r</i>	0.59	0.62	0.58	0.61	0.59	0.57	0.63
Wind speed							
<i>RMSE</i>	2.4	1.9	2.3	2.2	2.1	2.2	1.9
<i>IA</i>	0.46	0.49	0.48	0.48	0.47	0.46	0.52
<i>r</i>	0.18	0.17	0.23	0.23	0.19	0.18	0.23

*IA* value detects additive and proportional differences in the observed and simulated means and variances, however it is overly sensitive to extreme values due to squared differences (Legates and McCabe 1999).

All of the PBL schemes delivered relatively similar results. The *IA* value for temperature in the vertical statistics is 0.94–0.98, which is much higher than in the surface statistics, where the *IA* value is 0.83–0.90. The wind speed shows the opposite tendency, with *IA* values of 0.64–0.74 for the surface and *IA* values of 0.46–0.52 for vertical statistics, respectively. The *RMSE* values for temperature averaged for all PBL schemes are  $\approx 5$  °C (surface statistics) against  $\approx 2$  °C (vertical statistics). In contrast, *RMSE* values for wind speed are slightly higher for the vertical in comparison with surface statistics. The model data correlated better with the observations for the temperature than for the wind (especially for the vertical wind profile). Note that the vertical statistics are calculated at a single location (the SB site). The wind predictions are more difficult to evaluate using measurements taken at a single point, given the subgrid inhomogeneity of the velocity vector within a grid area, more so than with temperature. These statistics are not unexpected intuitively because at the surface the wind speed approaches zero, whereas the temperature has a maximum diurnal variation.

In general, the calculated meridional wind component is in better agreement with observations than is the zonal wind component, perhaps due to a well-developed valley flow captured by the model. In contrast, the zonal wind component is frequently affected by the interaction of slope and valley flows, which is due to intense flow collisions and the confluence of slope and valley flows (Fernando et al. 2015). Such processes are not included in current PBL parametrizations.

Overall, the performance of PBL schemes is expected to be sensitive to the basin configuration, since nuances of flow dynamics determine the efficacy of a particular PBL scheme. The QNSE scheme gives the best agreement with temperature observations (see *IA* values in Tables 1 and 2), whereas the YSUmod scheme is superior at forecasting the entire vertical

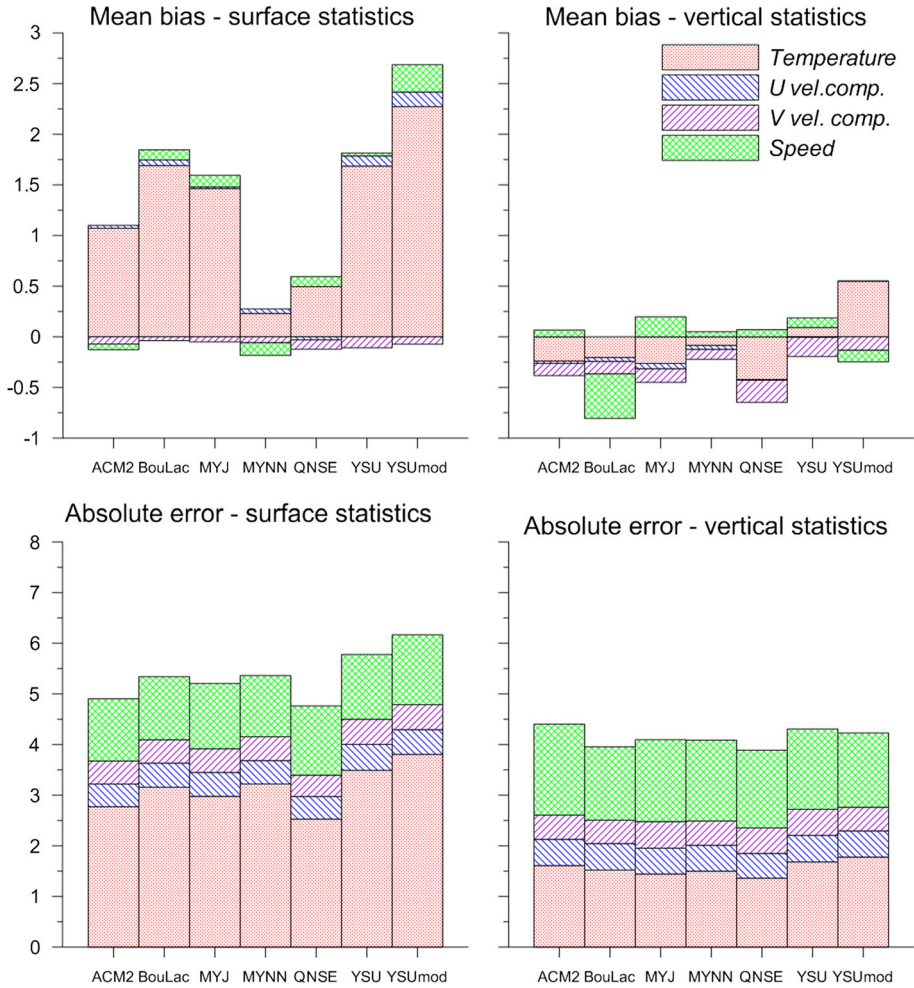


**Fig. 2** Mean biases and absolute errors from surface and vertical statistics

wind profile up to 400 m (see *IA* values in Table 2). There is a noticeable improvement in the predictions of the wind-speed vertical profile by the YSUmod scheme compared to the YSU scheme based on all statistical measures (see Table 2). The corresponding temperature prediction of the YSUmod scheme, however, leaves much to be desired. This, in part, can be attributed to the near-surface temperature bias, which concatenate with the prediction of temperature aloft through vertical transport processes.

In addition to the statistics shown in Tables 1 and 2, the mean biases and absolute errors for temperature and wind-speed are shown in Fig. 2. The mean biases for temperature at 2-m height are positive for all PBL schemes, which remain  $< 2.3\text{ }^{\circ}\text{C}$ . The biases are negative (except for YSU and YSUmod) for the entire layer up to 400 m. The mean biases for different PBL schemes vary according to the wind speed, and are  $< 0.5\text{ s}^{-1}$  (except for the BouLac scheme). The absolute error for temperature at 2 m ( $\approx 3\text{ }^{\circ}\text{C}$ ) is twice as great as the error calculated from the vertical profile ( $\approx 1.5\text{ }^{\circ}\text{C}$ ). The wind-speed absolute errors are similar for all PBL schemes and for both statistics ( $\approx 1.5\text{ m s}^{-1}$ ).

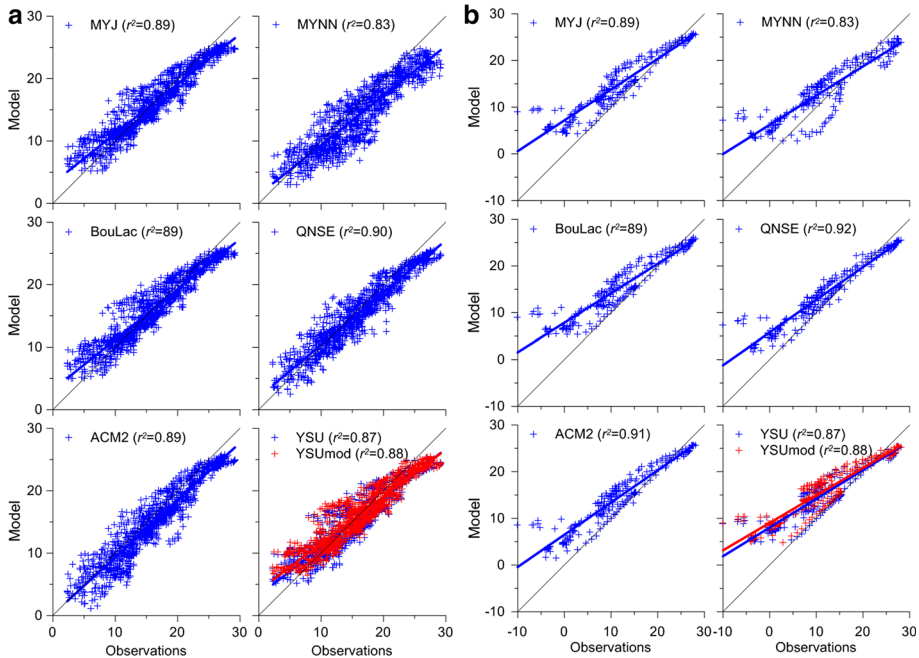


**Fig. 3** Scatter plots for temperature at the east slope—ES2, ES3, ES4, ES5 (**a**) and inside the valley—SB (**b**) towers

To further investigate the near-surface air temperature (at 2 m), a number of scatter plots are shown in Fig. 3. The data from the Granite mountain slope towers (ES2, ES3, ES4, ES5 towers) are all combined onto one series of scatter plots, while the SB tower data in the Dugway valley are shown separately. For all the PBL schemes, including the YSUmod scheme, the correlation of predictions with slope-flow observations is reasonably good (Fig. 3a). Some discrepancies are shown in predicting the extreme values. At the SB site, all of the PBL schemes substantially overestimate the minimum temperatures during the stably stratified period (Fig. 3b).

The evolution of potential temperature profiles are shown in Fig. 4, starting from just before sunset. All PBL schemes delay the development of the stably stratified layer inside the valley as compared to the observations, thus causing errors in the prediction of the stable boundary-layer height. It is also evident that the WRF model predicts the evening transition period poorly. The energy budget reverses above the valley surface when outgoing longwave radiation exceeds the incoming shortwave radiation, which first occurs in the late afternoon in areas shadowed by the terrain (Zardi and Whiteman 2013). With the reversal in sign of the net radiation the ground begins to cool, a downward turbulent sensible heat flux now exists, forming a shallow layer of cool air over the sidewalls and on the valley floor. The model generates the stable layer over the valley floor at a lower rate than in the field due to inadequate prediction of the air temperature at the first model level, which may be attributed in part to the inadequacies of the surface-layer schemes. It has been pointed out by Tastula et al. (2015a) that the choice of the surface-layer scheme significantly affects temperature predictions up to a height  $\approx 150$  m, irrespective of the number of vertical levels employed in the model.

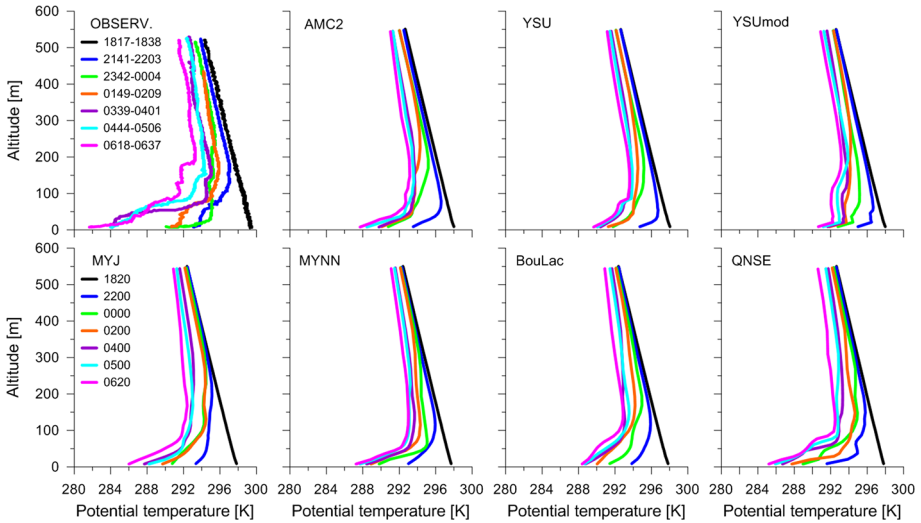


**Fig. 4** Nocturnal evolution of the potential temperature profiles inside the valley (at SB site) for IOP1 (28–29 September 2012)

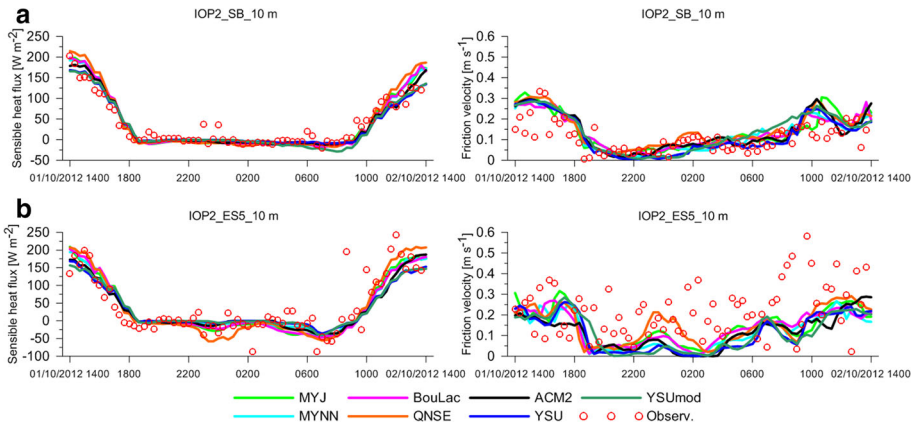


**Fig. 5** Sensible heat flux and friction velocity at SB (a) and ES5 (b) towers at the 10 m level for IOP2, October 1–2 2012

A comparison between several observed and predicted surface-flow characteristics are shown in Fig. 5 for the SB and ES5 towers. The observed friction velocity on the east slope is twice that of the valley floor (where strong stable conditions occur). All PBL schemes underestimate the friction velocity on the slope during the night. Substantial variations of the observed heat and momentum fluxes at the ES5 tower (Fig. 5b) can be linked to a variety of mechanisms, including sporadic canyon flows, flow oscillations and breakdown (Princevac et al. 2008); and periodic penetration of gap-flow effects (Fernando et al. 2015). Downslope flows often intrude into the valley, producing horizontal shears above or below the slope flows that vary with elevation and time. Such complexities in natural flows are not captured well by the model because of inadequate representation of topography, insufficient grid resolution and the difficulties of representing subgrid mixing processes.

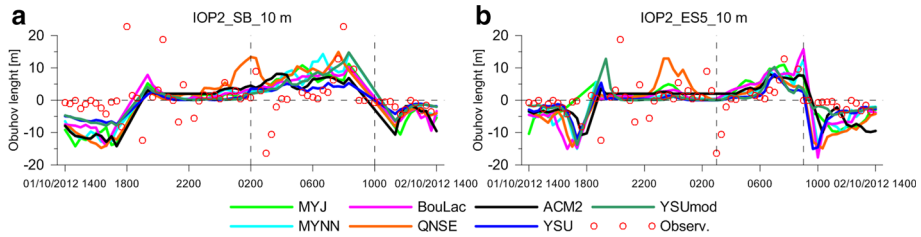


**Fig. 6** The Obukhov length at SB (a) and ES5 (b) towers at the 10-m level for IOP2 (October 1–2 2012). High values of  $L$  during the transition periods (morning and evening) are removed to make the figure more readable. The sign of  $L$  indicates unstable (–) or stable (+) conditions. The time shown is local

Although MOST is almost always employed for estimating near-surface fluxes (e.g. Stull 1988; Zilitinkevich et al. 2002), its usage is questionable for katabatic flows (e.g. Grisogono and Oerlemans 2001a, b) and other stable PBL flows (e.g. Mahrt 1999, 2007; Zilitinkevich and Calanca 2000; Jericević and Grisogono 2006; Zilitinkevich and Esau 2007). The Obukhov length ( $L$ ) calculated using field data at 10 m and that produced by different PBL schemes at the first model level inside the valley and on the east slope are shown in Fig. 6. The extreme values of  $L$  occurring in the morning and evening transition periods are not shown to ensure legibility of the figure. The time periods during which the model overestimates  $L$  during stable conditions are marked by dashed lines in Fig. 6. At both sites, the model-calculated  $L$  exceeds the observed  $L$  (calculated using 20-min averaging) during morning hours, especially at the SB tower.

Grachev et al. (2015) reported turbulence statistics (e.g., fluxes, variances, spectra, and co-spectra) of the katabatic winds measured at the same four towers as used in this study. The authors suggested that the position of the maximum jet speed of the katabatic flow can be derived from a linear interpolation between positive and negative values of the momentum (or the horizontal heat) flux and by determining the flux zero-crossing height. The height of the wind-speed maximum was found to be at  $\approx 3$  m. Profiles of turbulent fluxes and other quantities exhibited steep gradients below this maximum. The zero wind shear, change in the sign of vertical momentum flux, local minimum in TKE and dissipation rate, and the background stable stratification suggest that turbulence in the layer above the wind-speed maximum is decoupled from the surface. This case violates MOST, and  $L$  is too large to represent near-surface fluxes induced by a low-level katabatic jet.

All PBL schemes suitably capture the slope and valley flows (the diurnal thermal circulation is shown in Fig. 7). The valley flow is from the north-west during the daytime and from the south-east at night due to the orientation of the valley (Fig. 7a) while the upslope flow is easterly and the katabatic flow is westerly. The nocturnal flow at the SB site is better predicted than at the ES5 site (Fig. 7b).

Comparison of simulated vertical profiles of temperature, wind speed, and wind direction with the measurements at the SB site are shown in Fig. 8 for IOP8 (18 October, 2012). All of the schemes produce similar results for temperature, while all schemes are incapable of capturing the sharp temperature gradient observed close to the ground. The wind speeds of the nocturnal flow inside the valley were substantially underestimated, and the observed wind-speed maxima located at about 75 and 350 m above the ground level are not captured. The change of wind direction at the top of stably-stratified layer indicates an interface between air masses, across which turbulent mixing is weak. The best PBL scheme for predicting the near-surface temperature appears to be QNSE scheme that employs a surface-layer parametrization

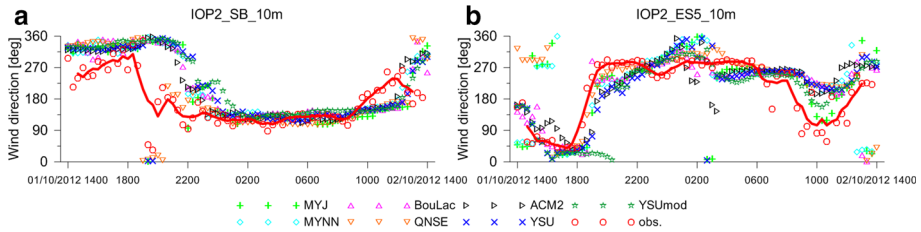


**Fig. 7** Wind direction at the SB (a) and ES5 (b) related to different PBL schemes for IOP2 (October 1–2 2012). The red line is a running averaged data with the window of 100 min. The time shown is local

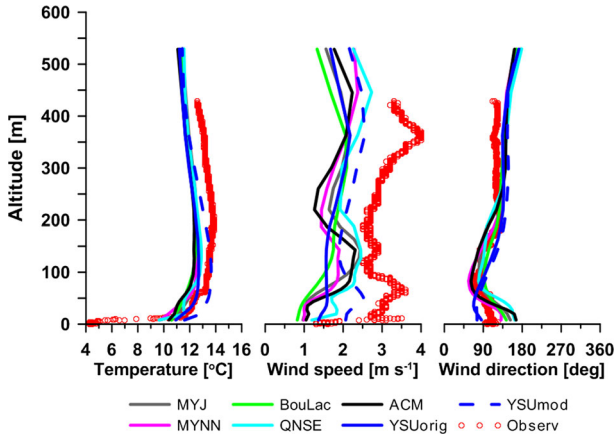


**Fig. 8** Comparison between different PBL schemes and tethered-balloon data at SB site for IOP8, October 18 2012 (tethered balloon ascent time 2203–2228; model output averaged from 2200–2220 local time)

based on spectral theory. However, predictions for wind are markedly different from the observed profiles at higher altitudes, possibly due to inadequacy of momentum transfer mechanisms encapsulated in the QNSE scheme (Tastula et al. 2015b). The authors found that the scheme exhibits vertical mixing that is too strong, and attributed to the applied TKE scheme and the stability functions. The 75-m jet-like structure lies just above the observed temperature inversion, with the damping of turbulence at this level leading to flow acceleration above the interface being unaffected by the surface-layer stresses. In order to capture this phenomenon, dynamics of the thin inversion ought to be well represented in the PBL scheme with sufficiently high vertical resolution. In spite of the fine vertical resolution (22 levels within the first 600 m), the model remains unable to capture the thin layers that occur inside the valley flow.

The YSUmod scheme reproduced vertical profiles of velocity and temperature reasonably well within the nocturnal PBL, at least in a qualitative sense, except at the lowest levels. The YSUmod scheme should be able to concentrate momentum near the top of the SBL and so develop a jet at that height, but the predicted height was somewhat lower than that observed. Missing physical representation of thin inversion layers that represents their ability to enhance momentum transfer through instabilities (Strang and Fernando 2001a), inadequate vertical resolution near the ground, as well as the overestimation of temperature at the first model level (that leads to an increase of temperature at model levels up to 50 m for this case), are all possible sources of prediction errors.

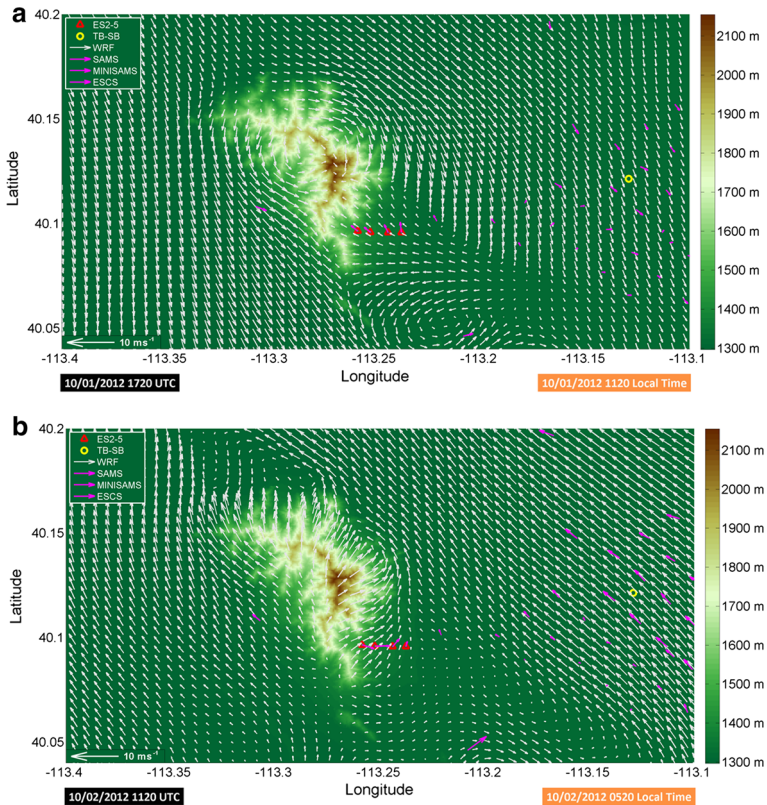


**Fig. 9** Wind vectors produced by the YSUmod scheme (*white*) compared with observations (*purple*) for IOP2, October 1–2 2012 during the day (**a**) and night (**b**)

The wind vectors for typical diurnal thermal circulation produced by the YSUmod scheme are shown in Fig. 9. The modified scheme captured the upslope/valley flow during daytime (Fig. 9a) and downslope/valley flow at night (Fig. 9b). The main model-data discrepancies are in the region where the valley and gap flows interact, which leads to drastic variability in the wind direction. This is most noticeable at night, where a layer of cold air from surrounding slopes becomes negatively buoyant and moves down the slopes, converges within the valley, interacts with the valley flow, and develops a strong directional shear. When the valley flow is sufficiently strong, the horizontal and vertical shear generate turbulence that can greatly modify the downslope flows (the ES3-ES5 tower data) or obliterate them entirely (the ES2 tower data).

#### 4.2 Sensitivity Tests of the YSU and YSUmod PBL Schemes to Grid Resolution

Sensitivity tests were conducted to assess the WRF model performance for three cases using different vertical and horizontal grid resolutions:

- 35 levels with 9 levels below 600 m and the first half level at approximately 17 m;
- 40 levels with 14 levels below 600 m and the first half level at approximately 9 m;
- 50 levels with 22 levels below 600 m and the first half level at approximately 9 m.

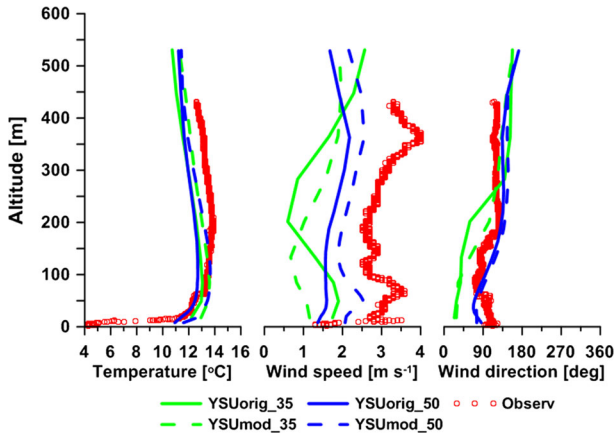


**Fig. 10** Comparison between the tethered-balloon data and both, original and modified schemes, using 35 and 50 vertical levels and 0.5-km grid at the SB site for IOP8, October 18 2012 (tethered balloon ascent time 2203–2228; model output averaged from 2200–2220 local time)

The primary goal was to test whether higher vertical resolution near the ground helps resolve the multi-layered nocturnal stably stratified structure. The increased vertical and horizontal resolution did not significantly change the temperature predictions. Minimal changes of temperature occurred due to the fact that the topography is almost uniform within the valley and the difference in land cover and ground properties over the grid was insignificant in each of the tested cases. The vertical temperature gradient is reasonably well captured by all PBL schemes (except close to the ground), and the number of vertical levels inside the mixing layer does not significantly affect vertical heat exchange (Fig. 10a).

In contrast, the modelled momentum flux is fairly dependent on the number of vertical levels, especially in the case of YSUmod scheme, with the predictions of this scheme agreeing better with observations than the other schemes (Fig. 10b, c). The *IA* values for wind speed were improved by increasing the vertical resolution, while decreasing the horizontal resolution (2 km) resulted in an improved *IA* values, possibly due to smoothing the outcome by eliminating sporadic fluctuations.

Increasing the number of vertical levels does not increase computational time substantially, therefore it does not affect the computational cost significantly. For example, computing time for IOP2 calculations increased from 16 h for 35 vertical levels to 17 h and 18 h for 40 and 50 levels, respectively (running on 12 cores).

WRF model results with the 0.5-km grid are better at capturing details on the slope, and within the gap (between Dugway range and Sapphire mountain) and the valley-flow interaction region, where the subgrid flow processes are intense. The comparison of wind vectors obtained with low (2-km) and high (0.5-km) grid spacing is shown in Fig. 11. The fine grid more robustly represents the flow modification in the zone of interaction between the downslope and valley flows, and the calculated wind speed accords better with the observations.

Calculations with a fine horizontal grid increase the computational expense considerably. For example, running only three domains results in computational time of 3 h; adding one more domain with 0.5-km grid spacing and  $145 \times 169$  points increases this time to 18 h using 12 cores.



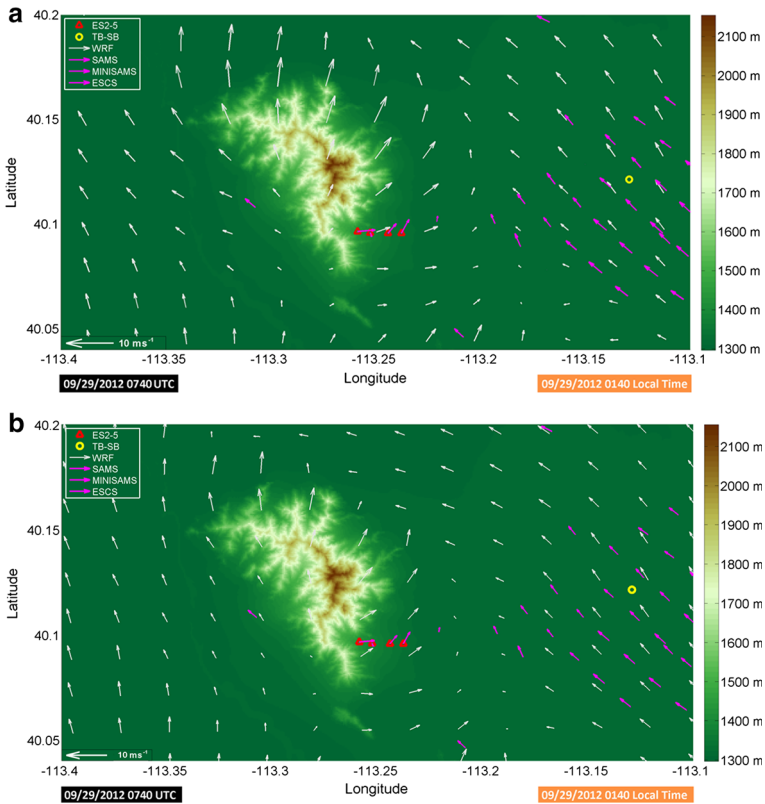


**Fig. 11** Wind vectors produced by the YSUmod scheme (*white*) compared with observations (*purple*) for IOP1, September 29 2012, at 0140 using 2 km (a) and 0.5 km (b) grids

### 5 Discussion and Conclusions

Our aim was to evaluate six different PBL closure schemes available in the Advanced Research version of the WRF model (ARW-WRFv3.4.1) using new high resolution data obtained during the MATERHORN field experiments. The experiments were conducted at the Granite Mountain Atmospheric Sciences Testbed of the US Army DPG during the autumn of 2012 and the spring of 2013. One of the PBL schemes used was the YSU scheme, which is reported to have performed well in previous studies of the CBL. Therefore, it was selected for further improvements to enhance prediction of the SBL by incorporating an alternative semi-empirical model for momentum and heat eddy diffusivities proposed by Monti et al. (2002). The resulting PBL scheme, the YSUmod scheme, allows momentum to diffuse more rapidly than heat at high Richardson numbers, and this permits a representation of internal-wave effects that are prevalent in the SBL. In the YSU scheme, the heat and momentum diffusivities in the SBL are set equal. In addition, the USGS 16-category database, together with a new parametrization for soil thermal conductivity in the Noah land-surface model for silt loam and sandy loam soils proposed by Massey et al. (2013), were used in an effort to reduce the nocturnal positive temperature bias in the study area. The main results are as follows:

- (i) All tested PBL schemes are found to be warm biased within the cold pool of the Dugway valley. The mean temperature bias and absolute errors in the surface layer are twice as much as those of the PBL aloft (based on surface and vertical statistics). The best PBL scheme for predicting the near-surface air temperature appears to be the QNSE scheme, which employs a surface-layer parametrization based on spectral theory. In this method, successive ensemble-averaging over infinitesimally thin spectral shells yields scale-dependent horizontal and vertical eddy diffusivities that account for transport processes on the eliminated scales; in so doing, the contribution of a mix of turbulence and internal waves is accounted for, and the spatial anisotropy of turbulent length scales is explicitly resolved.
- (i) The YSUmod scheme with an increased vertical resolution shows a general improvement in simulating velocity profiles in the PBL in comparison with the other tested schemes, in particular, away from the surface (above 50 m). The sensitivity to the vertical resolution, however, was smaller compared to that of the horizontal resolution. Even with a higher vertical resolution, a temperature inversion formed at a height of 75 m could not be resolved well by any of the PBL schemes. The relative success of the QNSE (see (i)) and YSUmod schemes implies that internal wave effects (e.g., different diffusivities of heat and momentum) ought to be accounted for in mesoscale modelling of the SBL.
- (ii) The surface-layer parametrizations significantly influence the prediction of the near-surface variability of temperature and velocity, specifically in the model layers closest to the ground. The errors generated propagate upward, effected through the PBL turbulent transport parametrizations. The coupling of the YSUmod scheme with a revised MM5 similarity surface-layer scheme employed in the original YSU scheme produced larger temperature biases compared to the original YSU scheme within the near-surface layer.
- (iii) The sharp temperature and wind-speed gradients observed near the ground could not be predicted by any of the parametrization schemes; as mentioned, the results of the QNSE scheme were closest to the observations. A possible explanation is the difficulties associated with MOST for stable cases, as MOST is used to specify the lower boundary conditions. In general, the measured Obukhov length was smaller than the first layer height, and thus within the first layer, buoyancy effects are more dominant than that specified in the model (considering that the Obukhov scale separates the regimes of mechanical and buoyancy dominated turbulence). This leads to the under-specification of the temperature gradient, which, in turn, leads to higher turbulent mixing rates by the PBL schemes and hence a positive temperature bias near the surface. In all, the present study calls for an improved methodology for treating the first model layer, which is important for successful predictions of meteorological profiles aloft under stable conditions.
- (iv) The meridional wind component was better predicted than the zonal component by all PBL schemes, reflecting the role of basin geometry. A well-developed valley flow was captured in simulations (meridional), but the slope flows (zonal) were modified by the interactions with the strong valley flow. In general, all PBL schemes poorly performed in regions where the valley flow interacts with the downslope and gap flows. Sporadic mixing events occurring during such interactions are not accounted for in the PBL schemes used, calling for the development of a conditional mixing parametrization that sets in when conditions conducive for specific mixing events emerge during simulations.

**Acknowledgments** This research was funded by the US Office of Naval Research Award # N00014-11-1-0709, Mountain Terrain Atmospheric Modelling and Observations (MATERHORN) Program. It has also been

supported by the European Union and the State of Hungary in the framework of TÁMOP-4.2.1.B-11/2/KMR-2011-0002 Instrument. Additional support was provided by the University of Notre Dame's Centre for Research Computing through computational and storage resources (we specifically acknowledge the assistance of Dodi Heryadi). Furthermore, we are thankful to Jeffrey Massey from the University of Utah for the updated land-cover and soil data.

## References

- Alapaty K, Pleim JE, Niyogi SR, Niyogi DS, Byun DW (1997) Simulation of atmospheric boundary layer processes using local and nonlocal-closure schemes. *J Appl Meteorol* 36:214–233
- Argüeso D, Hidalgo-Múnoz J, Gámiz-Fortis S, Esteban-Parra MJ, Dudhia J, Castro-Díez Y (2011) Evaluation of WRF parametrizations for climate studies over southern Spain using a multi-step regionalization. *J Clim* 24:5633–5651
- Awan N, Truhetz H, Gobiet A (2011) Parametrization induced error characteristics of MM5 and WRF operated in climate mode over the Alpine region: an ensemble based analysis. *J Clim* 24(12):3107–3123
- Borge R, Alexandrov V, del Vas JJ, Lumberras J, Rodriguez E (2008) A comprehensive sensitivity analysis of the WRF model for air quality applications over the Iberian Peninsula. *Atmos Environ* 42:8560–8574
- Bougeault P, Lacarrere P (1989) Parametrization of orography-Induced turbulence in a mesobeta-scale model. *Mon Weather Rev* 117(8):1872–1890
- Braun S, Tao W (2000) Sensitivity of high-resolution simulations of hurricane Bob (1991) to planetary boundary layer parametrizations. *Mon Weather Rev* 128(12):3941–3961
- Bright DR, Mullen SL (2002) The sensitivity of the numerical simulation of the southwest monsoon boundary layer to the choice of PBL turbulence parametrization in MM5. *Weather Forecast* 17(1):99–114
- Chen F, Dudhia J (2001) Coupling an advanced land surface-hydrology model with the Penn State-NCAR MM5 modelling system. Part I: model implementation and sensitivity. *Mon Weather Rev* 129:569–585
- Deng A, Stauffer D (2006) On improving 4-km mesoscale model simulations. *J Appl Meteorol* 45(3):361–381
- Doran JC, Fast JD, Horel J (2002) The VTMX 2000 campaign. *Bull Am Meteorol Soc* 83(4):537–551
- Dudhia J (1989) Numerical study of convection observed during the winter monsoon experiment using a mesoscale two-dimensional model. *J Atmos Sci* 46:3077–3107
- Evans J, Ekström M, Ji F (2011) Evaluating the performance of a WRF physics ensemble over south-east Australia. *Climat Dyn* 39:1241–1258
- Fernández J, Montávez J, Sáenz J, González-Rouco J, Zorita E (2007) Sensitivity of the MM5 mesoscale model to physical parametrizations for regional climate studies: annual cycle. *J Geophys Res* 112(D04101) doi:[10.1029/2005JD006649](https://doi.org/10.1029/2005JD006649)
- Fernando HJS (2003) Turbulence patches in a stratified shear flow. *Phys Fluids* 15(10):3164–3169
- Fernando HJS, Weil JC (2010) Whether the stable boundary layer? A shift in the research agenda. *Bull Am Meteorol Soc* 91(11):1475–1484
- Fernando HJS, Pardyjak ER (2013) Field studies delve into the intricacies of mountain weather. *EOS* 94(36):313–315
- Fernando HJS, Pardyjak ER, Di Sabatino S, Chow FK, DeWekker SFJ, Hoch SW, Hacker J, Pace JC, Pratt T, Pu Z, Steenburgh JW, Whiteman CD, Wang Y, Zajic D, Balsley B, Dimitrova R, Emmitt GD, Higgins CW, Hunt JCR, Kniewel JG, Lawrence D, Liu Y, Nadeau DF, Kit E, Blomquist BW, Conry P, Coppersmith RS, Creegan E, Felton M, Grachev A, Gunawardena N, Hang C, Hocut CM, Huynh G, Jeglum ME, Jensen D, Kulandaivelu V, Lehner M, Leo LS, Liberson D, Massey JD, McEnerney K, Pal S, Price T, Sghiatto M, Silver Z, Thompson M, Zhang H, Zsedrovič T (2015) The MATERHORN—unraveling the intricacies of mountain weather. *BAMS* <http://journals.ametsoc.org/doi/pdf/10.1175/BAMS-D-13-00131.1> (early online release)
- Flaounas E, Bastin S, Janicot S (2011) Regional climate modelling of the 2006 west african monsoon: sensitivity to convection and planetary boundary layer parameterisation using wrf. *Climat Dyn* 36(5):1083–1105
- Fry J, Xian G, Jin S, Dewitz J, Homer C, Yang L, Barnes C, Herold N, Wickham J (2011) Completion of the 2006 national land cover database for the conterminous United States. *Photogramm Eng Remote Sens* 77:858–864
- García-Díez M, Fernández J, Fita L, Yague C (2013) Seasonal dependence of WRF model biases and sensitivity to PBL schemes over Europe. *Q J R Meteorol Soc* 139(671):501–514
- Grachev A, Leo LS, Di Sabatino S, Fernando HJS, Pardyjak E, Fairall CW (2015) Structure of turbulence in katabatic flows below and above the wind-speed maximum. *Boundary-Layer Meteorol*. doi:[10.1007/s10546-015-0034-8](https://doi.org/10.1007/s10546-015-0034-8) (early online release)
- Grell GA, Dudhia J, Stauffer DR (1994) A description of the fifth-generation Penn State/NCAR mesoscale model (MM5). NCAR Technical Note: NCAR/TN-398+STR

- Grisogono B, Oerlemans J (2001a) Katabatic flow: analytic solution for gradually varying eddy diffusivities. *J Atmos Sci* 58:3349–3354
- Grisogono B, Oerlemans J (2001b) A theory for the estimation of surface fluxes in simple katabatic flows. *Q J R Meteorol Soc* 127:2725–2739
- Hong SY, Pan HL (1996) Nonlocal boundary layer vertical diffusion in a medium-range Forecast model. *Mon Weather Rev* 124(10):2322–2339
- Hong S, Noh Y, Dudhia J (2006) A new vertical diffusion package with an explicit treatment of entrainment processes. *Mon Weather Rev* 134(9):2318–2341
- Hu XM, Nielsen-Gammon JW, Zhang F (2010) Evaluation of three planetary boundary layer schemes in the WRF model. *J Appl Meteorol Climatol* 49:1831–1844
- Hunt JCR (1985) Diffusion in the stably stratified atmospheric boundary layer. *J Clim Appl Meteorol* 24:1187–1195
- Janjic Z (1990) The step-mountain coordinate: physics package. *Mon Weather Rev* 118:1429–1443
- Janjic ZI (1994) The step-mountain eta coordinate model: further development of the convection, viscous sublayer, and turbulence closure schemes. *Mon Weather Rev* 122:927–945
- Janjic ZI (2002) Nonsingular implementation of the Mellor–Yamada Level 2.5 Scheme in the NCEP Meso model, NCEP Office Note No 437
- Jankov I, Anderson CJ, Koch SE (2007) The impact of different physical parametrizations and their interactions on cold season QPF in the American River Basin. *J Hydrometeorol* 8:1141–1151
- Jericević A, Grisogono B (2006) The critical bulk Richardson number in urban areas: verification and application in a numerical weather prediction model. *Tellus* 58(1):19–27
- Jiménez PA, Dudhia J (2012) Improving the representation of resolved and unresolved topographic effects on surface wind in the wrf model. *J Appl Meteorol Climatol* 51(2):300–316
- Jiménez PA, Dudhia J, Gonzalez-Rouco JF, Navarro J, Montavez JP, Garcia-Bustamante E (2012) A revised scheme for the WRF surface layer formulation. *Mon Weather Rev* 140:898–918
- Kleczek M, Steeneveld GJ, Holtstg AAM (2014) Evaluation of the weather research and forecasting mesoscale model for GABLS3: impact of boundary-layer schemes, boundary conditions and spin-up. *Boundary-Layer Meteorol* 152:213–243
- Lee SM, Fernando HJS (2004) Evaluation of meteorological models MM5 and HOTMAC using PAFEX-I data. *J Appl Meteorol* 43(8):1133–1148
- Lee SM, Giori W, Princevac M, Fernando HJS (2006) Implementation of a stable PBL turbulence parameterization for the mesoscale model MM5: nocturnal flow in complex terrain. *Boundary-Layer Meteorol* 119:109–134
- Legates DR, McCabe GJ Jr (1999) Evaluating the use of “Goodness-of-fit” measures in hydrologic and hydroclimatic model validation. *Water Resour Res* 35(1):233–241
- LeMone MA, Tewari M, Chen F, Dudhia J (2013) Objectively determined fair-weather CBL depths in the ARW-WRF model and their comparison to CASES-97 observations. *Mon Weather Rev* 141(1):30–54
- Li X, Pu Z (2008) Sensitivity of numerical simulation of early rapid intensification of hurricane Emily (2005) to cloud microphysical and planetary boundary layer parametrization. *Mon Weather Rev* 136:4819–4838
- Lin YL, Farley RD, Orville HD (1983) Bulk parametrization of the snow field in a cloud model. *J Appl Meteorol* 22:1065–1092
- Massey J, Steenburgh WJ, Hoch SW, Kniviel JC (2013) Sensitivity of near-surface temperature forecasts to soil properties over a sparsely vegetated dryland region. *J Appl Meteorol Climatol* 53(8):1976–1995
- Mahrt L (1999) Stratified atmospheric boundary layers. *Boundary-Layer Meteorol* 90:375–396
- Mahrt L (2007) Bulk formulation of the surface fluxes extended to weak-wind stable conditions. *Q J R Meteorol Soc* 134(630):1–10
- Mahrt L (2010) Common microfronts and other solitary events in the nocturnal boundary layer. *Q J R Meteorol Soc* 136:1712–1722
- Mahrt L, Richardson S, Seaman N, Stauffer D (2012) Turbulence in the nocturnal boundary layer with light and variable winds. *Q J R Meteorol Soc* 138:1430–1439
- Mellor G, Yamada T (1982) Development of a turbulence closure model for geophysical fluid problems. *Rev Geophys Space Phys* 20(4):851–875
- Mlawer EJ, Taubman SJ, Brown PD, Iacono MJ, Clough SA (1997) Radiative transfer for inhomogeneous atmospheres: RRTM, a validated correlated-k model for the longwave. *J Geophys Res Atmos* 102(14):16663–16682
- Monin A, Obukhov A (1954) Basic laws of turbulent mixing in the atmospheric surface layer. *Trudy Geofizicheskogo Instituta Akademiiya Nauk SSSR* 24:163–187
- Monin A, Yaglom A (1965) Statistical fluid mechanics. In: *Mechanics of turbulence*, vol 1 (Translated from the Russian by Scripta Technica, Inc). MIT Press, Cambridge, 770 pp

- Monti P, Fernando HJS, Princevac M, Chan WC, Kowalewski TA, Pardyjak ER (2002) Observations of flow and turbulence in the nocturnal boundary layer over a slope. *J Atmos Sci* 59:2513–2534
- Nakanishi M, Nino H (2006) An improved Mellor\_Yamada level-3 model: its numerical stability and application to a regional prediction of advection fog. *Boundary-Layer Meteorol* 119:397–407
- Otkin J, Greenwald T (2008) Comparison of WRF model-simulated and MODIS-derived cloud data. *Mon Weather Rev* 136(6):1957–1970
- Pearson HJ, Puttock JS, Hunt JCR (1983) A statistical model of fluid element motions and vertical diffusion in a homogeneous stratified turbulent flow. *J Fluid Mech* 129:219
- Pleim JE (2006) A simple, efficient solution of flux-profile relationships in the atmospheric surface layer. *J Appl Meteorol Climatol* 45(2):341–347
- Pleim JE (2007a) A combined local and nonlocal closure model for the atmospheric boundary layer. Part I: model description and testing. *J Appl Meteorol Climatol* 46(9):1383–1395
- Pleim JE (2007b) A combined local and nonlocal closure model for the atmospheric boundary layer. Part II: application and evaluation in a mesoscale meteorological model. *J Appl Meteorol Climatol* 46(9):1396–1409
- Princevac M, Hunt JCR, Fernando HJS (2008) Quasi-steady katabatic winds over long slopes in wide valleys. *J Atmos Sci* 65:627–643
- Reeves HD, Stensrud DJ (2009) Synoptic-scale flow and valley cold pool evolution in the western United States. *Weather Forecast* 24:1625–1643
- Rife DL, Warner TT, Chen F, Astlin EG (2002) Mechanisms for diurnal boundary layer circulations in the Great Basin Desert. *Mon Weather Rev* 130:921–938
- Shin HH, Hong SY (2011) Intercomparison of planetary boundary-layer parametrizations in the WRF model for a single day from CASES-99. *Boundary-Layer Meteorol* 139:261–281
- Stensrud D, Weiss S (2002) Mesoscale model ensemble forecasts of the 3 May 1999 tornado outbreak. *Weather Forecast* 17(3):526–543
- Strang EJ, Fernando HJS (2001a) Entrainment and mixing in stratified shear flows. *J Fluid Mech* 428:349–386
- Strang EJ, Fernando HJS (2001b) Vertical mixing and transports through a stratified shear layer. *J Phys Oceanogr* 31:2026–2048
- Stull RB (1988) An introduction to boundary layer meteorology. Kluwer Academic Publishers, Dordrecht, 666 pp
- Sukoriansky S, Galperin B, Perov V (2005) Application of a new spectral theory of stably stratified turbulence to the atmospheric boundary layer over sea ice. *Boundary-Layer Meteorol* 117(2):231–257
- Sukoriansky S (2008) Implementation of the quasi-normal scale elimination (QNSE) model of stably stratified turbulence in WRF, Report on WRF-DTC Visit. [http://www.dtcenter.org/visitors/reports\\_07/Sukoriansky\\_report.pdf](http://www.dtcenter.org/visitors/reports_07/Sukoriansky_report.pdf). Accessed 08 Nov 2014
- Tastula EM, Galperin B, Sukoriansky S, Luhar A, Anderson P (2015a) The importance of surface layer parametrization in modeling of stable atmospheric boundary layers. *Atmos Sci Lett* 16:83–88
- Tastula EM, Galperin B, Dudhia J, LeMone MA, Sukoriansky S, Vihma T (2015b) Methodical assessment of the differences between the QNSE and MYJ PBL schemes for stable conditions. *Q J R Meteorol Soc*. doi:10.1002/qj.2503
- Wagner J, Gohm A, Rotach M (2014) The impact of horizontal model grid resolution on the boundary layer structure over an idealized valley. *Mon Weather Rev* 142:3446–3465
- Willmott CJ (1981) On the validation of models. *Phys Geogr* 2:184–194
- Zardi D, Whiteman CD (2013) Mountain weather research and forecasting, recent progress and current challenges. In: Chow FK, De Wekker SFJ, Snyder BJ (eds) *Diurnal mountain wind systems*, Chapter 2, Springer, Dordrecht, pp 35–121
- Zhang D, Anthes RA (1982) A high-resolution model of the planetary boundary layer—sensitivity tests and comparison with SESAME-79 data. *J Appl Meteorol* 21:1594–1609
- Zhang D, Zheng W (2004) Diurnal cycles of surface winds and temperatures as simulated by five boundary layer parametrizations. *J Appl Meteorol* 43(1):157–169
- Zhang H, Pu Z, Zhang X (2013) Examination of errors in near-surface temperature and wind from WRF numerical simulations in regions of complex terrain. *Weather Forecast* 28(3):893–914
- Zhong S, Fast J (2003) An evaluation of the MM5, RAMS, and Meso-Eta models at subkilometer resolution using VTMX field campaign data in the Salt Lake Valley. *Mon Weather Rev* 131:1301–1322
- Zilitinkevich S, Calanca P (2000) An extended theory for the stably stratified atmospheric boundary layer. *Q J R Meteorol Soc* 126:1913–1923
- Zilitinkevich S, Baklanov A, Rost J, Smedman AS, Lykosov V, Calanca P (2002) Diagnostic and prognostic equations for the depth of the stably stratified Ekman boundary layer. *Q J R Meteorol Soc* 128:25–46
- Zilitinkevich S, Esau I (2007) Similarity theory and calculation of turbulent fluxes at the surface for the stably stratified atmospheric boundary layer. *Boundary-Layer Meteorol* 125:193–205